# Preparation of Gold Nanoparticles on Nanocellulose and their Catalytic Activity for Reduction of NO$_2^-$

Zihe Guo and Shiyu Fu *

Nanoscale material has attracted the interest of many researchers because of its special physicochemical and surface properties. In this study, a nanocomposite was prepared based on cellulose nanocrystals (CNCs) *in situ* forming ultra-fine size gold nanoparticles. To form the gold nanoparticles, chloroauric acid was reduced with an aqueous mixture of ethanol and CNC. The gold nanoparticles were less than 8 nm in size, with 80% of them less than 5 nm. Nanocellulose in the preparation system acted as a stabilizer. The size and dispersity of the ultra-fine gold nanoparticles (UAuNPs) were controlled by adjusting the pH. The resulting UAuNPs/CNCs composite exhibited excellent catalytic performance to eliminate solubilized NaNO$_2$ mixed with NH$_4$Cl at room temperature. The apparent rate constant of the reaction was 4.12 × 10$^{-5}$ s$^{-1}$. The catalytic effect of the generated UAuNPs on NO$_2^-$ reduction has potential use in many fields, particularly in the food and environmental sectors.

*Contact information: State Key Laboratory of Pulp and Paper Engineering, South China University of Technology, Guangzhou, China; *Corresponding author: shyfu@scut.edu.cn*

## INTRODUCTION

Gold is a useful element for chemists because it can be made into special functional materials of various shapes. Nanoparticles and self-assembled monolayers (SAMs) comprised of gold are some of the emerging applications in the field of nanoscience and nanotechnology (Bumbudsanpharoke and Ko 2015). Gold nanoparticles (AuNPs) refer to nanosized gold particles with a large specific surface area, high surface energy, and high activity for catalytic reactions. These AuNPs exhibit unique physical and chemical properties that bulk gold does not possess. The surface effect, surface plasmon resonance effect, and quantum size effect are some of the unique effects from AuNPs (Halperin 1986; Daniel and Astruc 2004; Ghosh and Pal 2007). Due to their unique properties, AuNPs are widely applied in many areas such as industrial catalysis, biological medicine, biological analytical chemistry, and rapid detection (Panigrahi *et al.* 2007; Ai *et al.* 2009; Marques *et al.* 2016; Paukkonen *et al.* 2017). Both physical and chemical methods can be used to fabricate AuNPs. Physical methods such as vacuum evaporation, soft landing, and laser ablation can produce high quality gold particles with few impurities (Veith *et al.* 2005). However, physical methods are costly and require special equipment. Additionally, physical fabrication methods do not provide much control over the size and shape of the AuNPs. Some of the main chemical methods include sodium citrate reduction, crystal seed growth, two-phase method, and self-assembly. The resulting AuNPs from chemical methods are too large for many applications, have uneven size distribution of particles, and tend to exhibit agglomeration

of particles.

The most widely used method for AuNPs production is the self-assembly of the gold atom by reducing chloroauric acid with ethanol, which may affect the size of the AuNPs. The most established and widely used reduction method is the sodium citrate reduction method proposed by Turkevich many years ago (Turkevich *et al.* 1951). When sodium citrate reduction is used to prepare AuNPs, the sodium citrate acts as both a reducing agent to obtain spherical AuNPs and as a protective agent to stabilize the AuNPs. Adjusting the ratio of sodium citrate and chloroauric acid has been shown to produce AuNPs 16 to 147 nm in size (Frens 1973). Polyethylene glycol (PEG) was used as a reductant to prepare 15 to 25 nm AuNPs, which were applied to reduce p-nitro-toluene (Yan *et al.* 2016).

When CNCs were used as a reducing agent and stabilizer, AuNPs of approximately 25 nm were produced with a good photothermal effect (Hu *et al.* 2017a,b). In the above reaction system, the prepared AuNPs need stabilizing agents such as PEG, CNC, carbon, silicon, or metal oxides because AuNPs alone are unstable and easily aggregate in the solution due to the van der Waals forces. Compared to other agents, CNCs are natural and biodegradable (Xu *et al.* 2017), while exhibiting excellent performance properties such as high crystallinity, high purity, high Young's modulus, high hydrophilicity, ultra-fine structure, and high transparency (Abdul Khalil *et al.* 2012; Mittal *et al.* 2017). Nevertheless, monofunctional nanofillers only improve upon a specific property for host matrices, whereas multifunctional nanofillers can provide multiple properties for the resulting nanocomposites.

Cellulose nanocrystals can function as stabilizers, dispersants, and templates for the carrying of gold nanoparticles (Hajian *et al.* 2017; Xiong *et al.* 2018). For example, Zhang *et al.* (2018) succeeded in synthesizing palladium and gold nanoparticles by using dialdehyde nanocellulose as a template and reducing agent. Similarly, Koga *et al.* (2010) synthesized *in situ* highly dispersed AuNPs on the surface of 2,2,6,6-tetramethylpiperidinyl-1-oxyl free radical (TEMPO)-oxygenized cellulose nanofibers in the presence of $NaBH_4$. The prepared AuNPs on carriers were applied in catalysis for oxidation or reduction because of the surface effect of AuNPs with high surface energy and surface binding energy, which refers to the nanoparticles distinguished from the body of gold (Lopez *et al.* 2004). Specific surface area refers to the total area of a unit mass of material. The prepared AuNPs are spheroidal. Therefore, the smaller the particle size of the AuNPs, the larger the specific surface area and the larger the surface energy and surface binding energy.

Gold nanoparticles with a diameter of less than 5 nm are defined here as ultra-fine gold nanoparticles (UAuNPs). When the diameter of the gold particles is 1 nm, UAuNPs are formed and the specific surface area is the largest. At this point, the surface energy and surface binding energy of the UAuNPs are greatly increased, leading to a significant improvement in the catalytic performance of UAuNPs.

Due to their high surface energy and surface binding ability, UAuNPs have high activity for catalysis. These properties allow UAuNPs/CNCs to catalyze the reduction of nitrite with $NH_4Cl$, which takes place in the laboratory to produce nitrogen or to remove nitrite. Usually, this reaction should be carried out at 60 °C or above. When UAuNPs are used as a catalyst, the reaction can happen at room temperature with a second-order. This catalytic reaction can potentially be applied to remove nitrite substances in food.

*bioresources.com*

## EXPERIMENTAL

### Materials

Cotton linters with a moisture content of 8% were supplied by Fumin Chemical Fiber Co. Ltd. (Shandong, China). Analytical grades of sulfuric acid (98 wt. %), sodium hydroxide, gold(III) chloride trihydrate, anhydrous ethanol, ammonium chloride, and sodium nitrite were purchased from the Guangzhou Chemical Reagent Factory (Guangzhou, China). All chemicals were used as received.

### Preparation of CNCs

Cellulose nanocrystals were prepared from cotton linters by acid hydrolysis according to a previously reported method (Tian *et al.* 2014). A quantity of 64 wt% $H_2SO_4$ and dry cotton linters were added in a ratio of 13.5 to 1 (w/w). The mixture was stirred at 45 °C for 90 min, then diluted 10 times to terminate the reaction with water. After centrifugation washing two to three times, the reaction solution was dialyzed for two to three days until the pH was neutral. Finally, a uniform CNC was obtained by ultra-sonication at 40 °C for 3 min and stored at 4 °C.

### Preparation of CNCs-Supported UAuNPs Suspensions (UAuNPs/CNCs)

A modified method was used to prepare UAuNPs in the presence of CNCs (Hu *et al.* 2017b). A 5 mL quantity of anhydrous ethanol and 542 μL of $HAuCl_4$ (9.71 mM) were added to a 50 mL CNC (0.5 wt%) suspension at 70 °C under constant magnetic stirring for 45 min. The pH was set at 12 and was adjusted by using 0.5 M NaOH. The UAuNPs/CNCs suspension contained 20.74 ppm of UAuNPs and was stored at 4 °C for further use.

### Characterization of UAuNPs/CNCs Nanocomposites

X-ray diffraction (XRD) patterns of freeze-dried AuNP/CNCs were collected on a D8 Advance X-ray Diffractometer (Bruker Corporation, Karlsruhe, Germany) using Ni-filtered Cu KR radiation ($\lambda$ = 0.154 18 nm) at 40 kV and 20 mA. Data were collected over the 2$\theta$ range of 5 to 90° with a scan step size of 0.04° at a rate of 1° per min. Ultraviolet-visible (UV-Vis) absorption spectra from 400 to 1000 nm were obtained using an Agilent Technologies HP-8453 spectrophotometer (Santa Clara, CA, USA) with deionized water as the blank.

The morphologies and sizes of the gold nanoparticles were observed by transmission electron microscopy (TEM) (H-7650, Hitachi, Japan) at 80 kV accelerating voltage. Atomic force microscopy (ATM) images of the AuNP/CNC nanocomposite films were recorded on a Bruker Multimode 8 atomic force microscope.

### Catalytic Reaction of NH₄Cl and NaNO₂

The reaction of $NH_4Cl$ and $NaNO_2$ can produce $N_2$, $H_2O$, and NaCl under suitable conditions. In the reaction, 20 mL of UAuNPs/CNCs suspension (total amount of UAuNPs: 0.002 mM) were added into the mixture of 0.05 M $NH_4Cl$ and 0.05 M $NaNO_2$ at 25 °C with constant stirring. Nitrogen gas produced over time was collected to determine the reaction rate.

## RESULTS AND DISCUSSION

### Preparation of UAuNPs/CNCs Nanocomposites

The prepared AuNPs samples have potential use in catalysis and photothermal effect materials (Panigrahi *et al.* 2007; Zhang *et al.* 2017). When CNCs were used as the scaffold and reducer of AuNPs, the AuNPs/CNCs composite was formed through the photothermal effect, as observed in previous research (Hu *et al.* 2017b). When ethanol was used as the reducing agent, an ultra-fine gold nanoparticle (UAuNP) suspension was obtained in the presence of CNC at pH 11.47. The UAuNP sample was 10 nm in size. The XRD spectra of the CNCs and UAuNP/CNC nanocomposites can be seen in Fig. 1. The results from Fig. 1 indicate that the CNC had a typical cellulose I structure with characteristic peaks of $2\theta$ angles at 15.1°, 22.5°, and 34.5°. Compared with CNC, the UAuNPs/CNCs had five extra diffraction peaks at $2\theta$ angles of approximately 38.1°, 44.1°, 64.6°, 77.4°, and 81.7°. These extra peaks were indexed as the 111, 200, 220, 311, and 222 lattice planes of the standard face-centered cubic phase of metallic gold, further indicating the formation of crystalline gold (Arockiya Aarthi Rajathi *et al.* 2014; Shi *et al.* 2015).
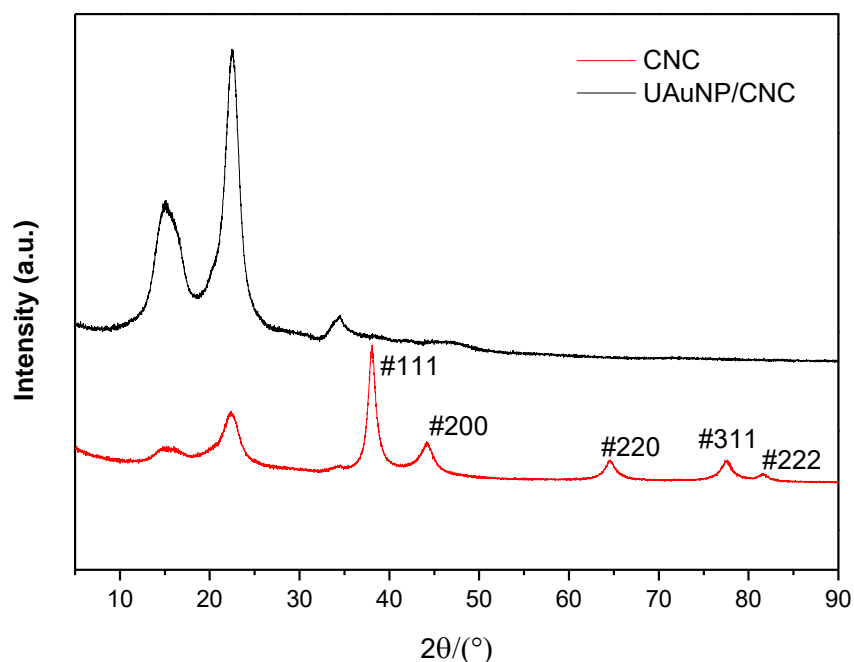


**Fig. 1.** X-ray diffraction patterns of CNCs and UAuNP/CNC nanocomposites

The particle size and crystalline gold structure were analyzed through AFM and TEM imagery. The AFM image of the UAuNP/CNC nanocomposite and the TEM images of the UAuNP/CNC nanocomposites are shown in Fig. 2. In Fig. 2a, the rod-like shape substances were CNCs 100 to 300 nm in length and 10 to 30 nm in width. The UAuNPs were uniformly dispersed on the well-dispersed CNCs. The crystal diffraction and shape of CNCs in Fig. 1 were in agreement with the previous results from many reports, which indicates that CNCs act as carriers for UAuNPs and do not change physically (Arockiya Aarthi Rajathi *et al.* 2014; Shi *et al.* 2015). It is probable that the reductive end of the cellulose molecule on the surface of the cellulose crystal was

oxidized to the carboxyl group by gold(III) during the reaction. The formed carboxyl group may provide negative charges that are beneficial for the dispersal of CNCs, as seen by the well dispersed CNCs in Fig. 2a. Figures 2b and 2d show the size and crystal diffraction pattern of the UAuNPs. Figure 2c illustrates that the visible particles originated from gold crystal. The distribution of the small particles was very even, as can be seen in Fig. 2d. When the viewing area in Fig. 2b was magnified, it was apparent that all of the gold particles in the darker area were less than 5 nm in size. To determine which particles in the darker areas were gold, the crystal diffraction pattern of the particles was measured, as shown in Fig. 2c. The diffraction pattern of the measured particles matched that of typical gold crystal, confirming that the particles were UAuNPs. While many previous studies have prepared gold nanoparticles, this was the first time that ultra-fine gold nanoparticles have been achieved. Yan *et al.* prepared 15 to 25 nm AuNPs using PEG as a reductant (2016). Siddiqi and Husen (2017) produced gold nanoparticles of about 25 nm in size and studied their application in biological systems. Chen *et al.* (2015) made AuNP/AOBC composites larger than 10 nm and applied them to the catalysis. Zhang and Zhao (2013) prepared AuNPs of about 10 nm in size and used them to make shape memory materials. There was no published research on the use of CNCs as a substrate and ethanol as a reducing agent to obtain UAuNPs through pH adjustment.
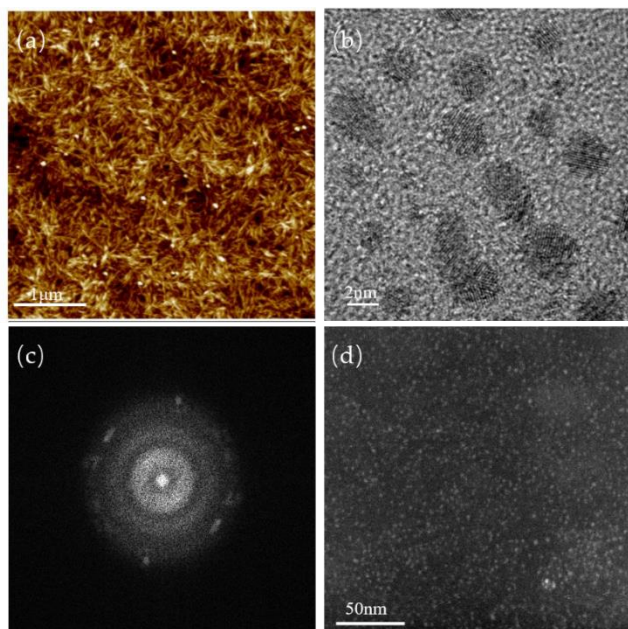


**Fig. 2.** The AFM images of (a) of the UAuNP/CNC nanocomposites and (b, c, d) the TEM images of the UAuNP/CNC nanocomposites

## Effects of pH to the Size of UAuNPs Schemes

Due to the surface plasmon resonance (SPR) absorption, gold nanoparticles have brilliant colors. Therefore, when $HAuCl_4$ was reduced with ethanol, the formed gold nanoparticle solution appeared magenta, as shown in Fig. 3. The color of the nanoparticle depends on the shape and size of the nanoparticle and dielectric constant of the surrounding medium. Many studies on the synthesis and application of colored nanoparticles have been conducted (Shi *et al.* 2015; Zhang *et al.* 2017). The changes in the $\lambda_{max}$ and SPR bandwidths characterized by the UV-Vis absorption spectra can be used

to explain the quantity and size of UAuNPs. Figure 4 illustrates the UV-Vis spectra of the UAuNP/CNCs nanocomposites at different pH levels under the same conditions. As the pH was increased from 4.47 to 12.50, a blue shift of the UV spectrum occurred, indicating that the size of the UAuNPs decreased. As the pH of the reaction medium increased, the SPR bands narrowed substantially, indicating that both the general monodispersity and homogeneity of the UAuNPs were improved (Leng *et al.* 2015).

The calculated particle size can be seen in Table 1, which indicates that UAuNPs with an average size of 4.8 nm were obtained at a pH of 12. The TEM images in Fig. 5 further demonstrate the change in size and shape of UAuNPs. When the reaction took place under acidic conditions (pH 4.47), the gold nanoparticles agglomerated, creating irregularly shaped particles. This is the result of the lower pH, which causes protonation of the carboxyl groups on the CNCs, resulting in the reduction of electrostatic repulsion. Under alkaline conditions, the generated UAuNPs were distributed evenly. From Fig. 5, it was found that the particle size of the obtained UAuNPs gradually decreased from 10 to 3 nm as the pH was changed from 10 to 12. The particle size of the UAuNPs reached their minimum when the pH was raised to 12. However, when the pH is too high, the opposite result is produced. So when pH rises to 12.5, the particle size increases again.



**Fig. 3.** The solution of the UAuNP/CNC
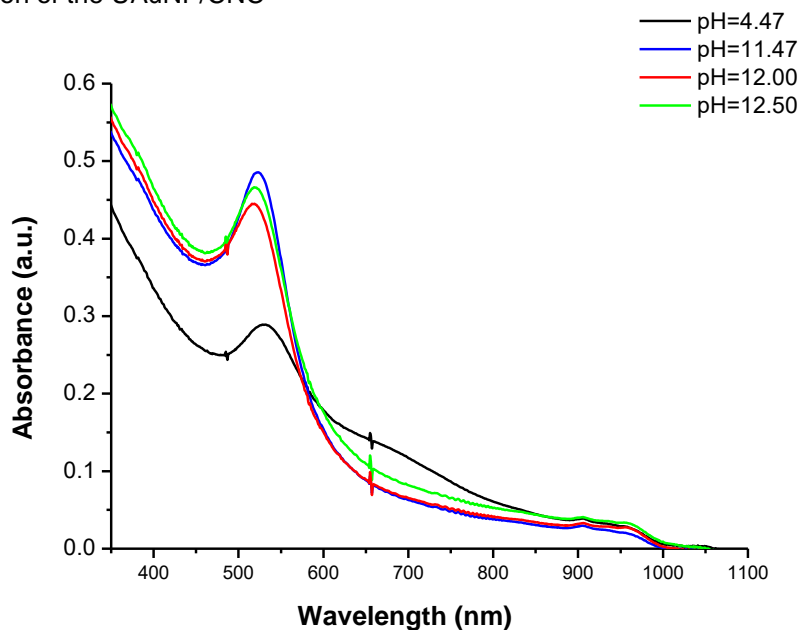


**Fig. 4.** UV-Vis absorption spectra of AuNPs prepared at various pH levels (4.47, 11.47, 12.00, and 12.50) with 0.2 mM $HAuCl_4$ and 0.5 M CNC
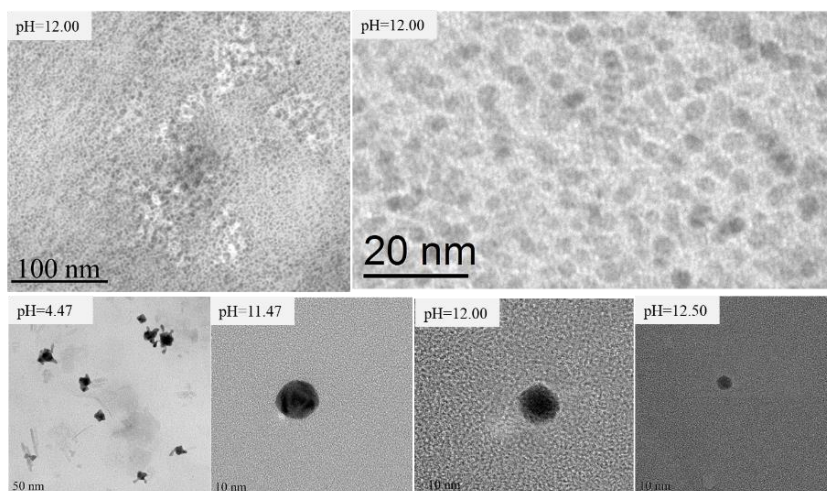
**Fig. 5.** The TEM images of the UAuNP/CNC nanocomposites prepared at various pH levels (4.47, 11.47, 12.00, and 12.50) with 0.2 mM $HAuCl_4$ and 0.5 M CNC

**Table 1.** Average Diameters and Maximum Absorbance Wavelength ($\lambda_{max}$) of the UAuNPs Prepared at Various pH Levels

| pH | $\lambda_{max}$ (nm) | Average Diameter (nm) |
|---|---|---|
| 4.47 | 531 | 23.4 |
| 11.47 | 517 | 11.6 |
| 12.00 | 519 | 4.8 |
| 12.50 | 521 | 13.7 |

## Catalytic Applications of UAuNPs/CNCs for Nitrite Removal

Nitrite in food is toxic to the human body. This is because if nitrite enters the human body in a large amount, it may cause "methemoglobinemia", and the blood loses the ability to carry oxygen, resulting in hypoxia symptoms, which may be life-threatening. So it should be removed. A typical reaction of $NaNO_2$ and $NH_4Cl$ produces nitrogen when the temperature is over 70 °C. Herein, the reaction could proceed at room temperature when UAuNPs were used as the catalyst. As shown in Fig. 6a, 10 mL of 0.5 mol/L $NaNO_2$ and $NH_4Cl$ were mixed in a conical flask at room temperature. No $N_2$ bubbles appeared at the bottom of the flask. However, when 10 mL of the UAuNP/CNC solution was added to the same mixture, bubbles arose from the solution at room temperature, as shown in Fig. 6b. This experiment demonstrated that UAuNPs catalyzed the reaction of $NaNO_2$ and $NH_4Cl$ at room temperature.
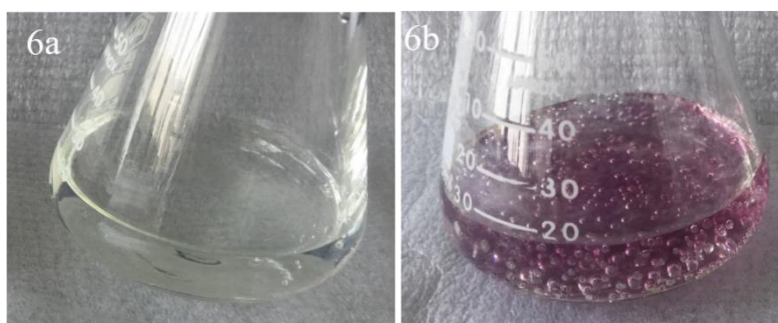


**Fig. 6.** Reaction of $NaNO_2$ with $NH_4Cl$ (a) in the absence of UAuNPs/CNCs and (b) in the presence of UAuNPs/CNCs

The catalytic action of UAuNPs/CNCs was demonstrated in further experiments, which are shown in Fig. 7. Nitrogen gas was collected using the gas-collecting method of drainage water, as can be seen in Fig. 7a. The amount of $N_2$ generated from the reaction was collected over the duration of the experiment.

(7a)



(7b)



$$1/c_A - 1/c_{A0} = 4.12*10^{-5}x + 1.52*10^{-4}$$
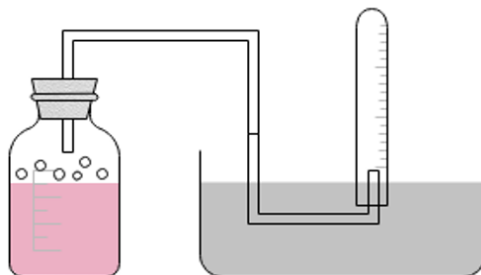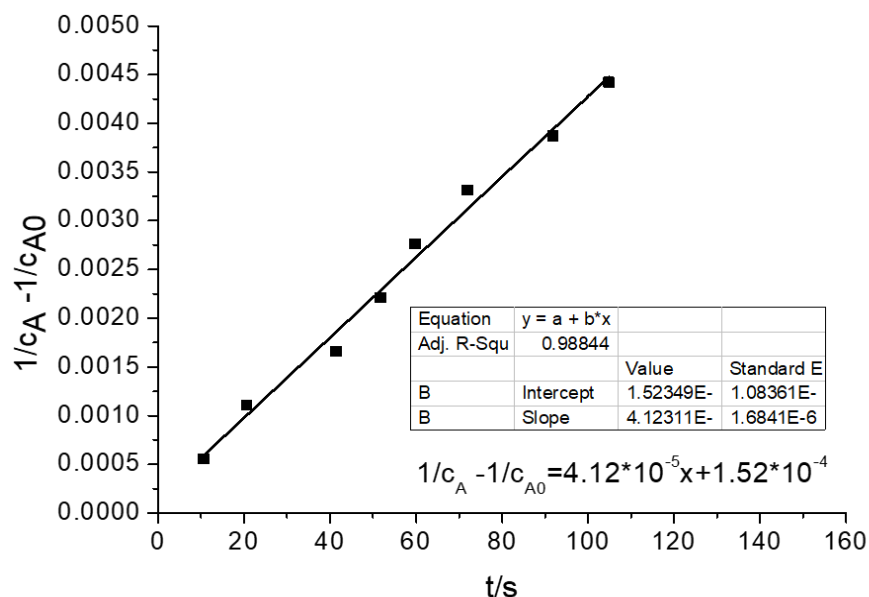
**Fig. 7.** (a) Reaction device schematic of $NaNO_2$ and $NH_4Cl$ using UAuNPs/CNCs as the catalyst and (b) $\frac{1}{c_A} - \frac{1}{c_{A0}}$ second order reaction diagram of $NaNO_2$

According to the simple chemical reaction rate equation, the index of each reactant concentration is referred to as the reaction order of the reactants. Based on the measured time required to generate a certain amount of $N_2$, the reaction order of the reaction can be determined. Quantities of 10 mL of 0.1 mol/L $NaNO_2$, 10 mL of 0.1 mol/L $NH_4Cl$, and 20 mL of 0.1 mM/L UAuNPs/CNCs were added to the conical bottle. The total concentration of UAuNPs was 10.37 ppm. The chemical reaction that occurred in the vessel is described by Eq. 1.

$$NO_2^- + NH_4^+ \rightarrow N_2 + 2H_2O \tag{1}$$

Table 2 shows the volume over time of $N_2$ production. As shown in Fig. 7b, $t$ was plotted on the abscissa and $(\frac{1}{c_A} - \frac{1}{c_{A0}})$ was plotted on the ordinate. Figure 7b shows that there was a linear relationship between $t$ and $(\frac{1}{c_A} - \frac{1}{c_{A0}})$, which proved that this reaction was a second order reaction and in accordance with Eq. 2.

$$\left(\frac{1}{c_A} - \frac{1}{c_{A0}}\right) = kt + b \tag{2}$$

The slope of the line provided the reaction rate. The solution after the reaction still exhibited the color of the UAuNPs. The UV-Vis absorption of the solution after the reaction still showed a peak of UAuNPs, confirming their existence. The UAuNPs/CNCs can be precipitated by centrifugation and separated from the supernatant, indicating that the UAuNPs/CNCs can be recycled and reused.

**Table 2.** Amount of $N_2$ Collected over Time and the Determination of $\frac{1}{c_A} - \frac{1}{c_{A0}}$

| $t$ (s) | Volume of $N_2$ (mL) | $\frac{1}{c_A} - \frac{1}{c_{A0}}$ |
|---|---|---|
| 10.63 | 1 | $5.52 \times 10^{-4}$ |
| 20.63 | 2 | $1.11 \times 10^{-3}$ |
| 41.47 | 3 | $1.66 \times 10^{-3}$ |
| 51.75 | 4 | $2.21 \times 10^{-3}$ |
| 59.77 | 5 | $2.76 \times 10^{-3}$ |
| 71.99 | 6 | $3.32 \times 10^{-3}$ |
| 91.87 | 7 | $3.87 \times 10^{-3}$ |
| 104.83 | 8 | $4.42 \times 10^{-3}$ |

Although elemental gold is often used as a catalyst for redox reactions, its catalytic efficiency is much higher when prepared as a nanoparticle. It is very efficient to reduce *p*-nitrotoluene with $NaBH_4$ when AuNPs are used as the catalyst (Koga *et al.* 2010; Yan *et al.* 2016). Biella *et al.* (2002) chose AuNPs to catalyze the selective oxidation of glycol with good results. Milone *et al.* (2001) oxidized salicylic alcohol to salicylaldehyde under the co-catalysis of gold and iron oxide. After surveying the literature, this is the first time that UAuNPs/CNCs composites have been implemented for the catalytic reduction of $NaNO_2$ in mild reaction conditions. The biggest advantage is that a trace amount of catalyst can achieve the desired effect and the catalyst can be recycled. This has great application prospects in food safety and environmental protection.

## CONCLUSIONS

1. When the pH was adjusted from 4.47 to 12, the obtained particle size became smaller, and the UAuNPs were better dispersed. Most of the UAuNPs were less than 5 nm at pH 12.

2. Applied CNCs acted as a good dispersant and stabilizer for the preparation of UAuNPs by reducing chloroauric acid with ethanol under alkaline conditions.

3. The UAuNPs produced by this method exhibited good catalytic activity, illustrating their use as a catalyst to accelerate the reaction of $NaNO_2$ and $NH_4Cl$ at room temperature.

## ACKNOWLEDGMENTS

## REFERENCES CITED

Abdul Khalil, H. P. S., Bhat, A. H., and Ireana Yusra, A. F. (2012). "Green composites from sustainable cellulose nanofibrils: A review," *Carbohydrate Polymers* 87(2), 963-979. DOI: 10.1016/j.carbpol.2011.08.078

Ai, K., Liu, Y., and Lu, L. (2009). "Hydrogen-bonding recognition-induced color change of gold nanoparticles for visual detection of melamine in raw milk and infant formula," *Journal of the American Chemical Society* 131(27), 9496-9497. DOI: 10.1021/ja9037017

Arockiya Aarthi Rajathi, F., Arumugam, R., Saravanan, S., and Anantharaman, P. (2014). "Phytofabrication of gold nanoparticles assisted by leaves of *Suaeda monoica* and its free radical scavenging property," *Journal of Photochemistry and Photobiology B: Biology* 135, 75-80. DOI: 10.1016/j.jphotobiol.2014.03.016

Biella, S., Castiglioni, G. L., Fumagalli, C., Prati, L., and Rossi, M. (2002). "Application of gold catalysts to selective liquid phase oxidation," *Catalysis Today* 72(1), 43-49. DOI: 10.1016/S0920-5861(01)00476-X

Bumbudsanpharoke, N., and Ko, S. (2015). "In-situ green synthesis of gold nanoparticles using unbleached kraft pulp," *BioResources* 10(4). DOI: 10.15376/biores.10.4.6428-6441

Chen, M., Kang, H., Gong, Y., Guo, J., Zhang, H., and Liu, R. (2015). "Bacterial cellulose supported gold nanoparticles with excellent catalytic properties," *ACS Applied Materials & Interfaces* 7(39), 21717-21726. DOI: 10.1021/acsami.5b07150

Daniel, M. C., and Astruc, D. (2004). "Gold nanoparticles: Assembly, supramolecular chemistry, quantum-size-related properties, and applications toward biology, catalysis, and nanotechnology," *Chemical Reviews* 104(1), 293-346. DOI: 10.1021/cr030698+

Frens, G. (1973). "Controlled nucleation for the regulation of the particle size in monodisperse gold suspensions," *Nature Physical Science* 241(105), 20-22. DOI: 10.1038/physci241020a0

Ghosh, S. K., and Pal, T. (2007). "Interparticle coupling effect on the surface plasmon resonance of gold nanoparticles: From theory to applications," *Chemical Reviews* 107(11), 4797-4862. DOI: 10.1021/cr0680282

Hajian, A., Lindström, S. B., Pettersson, T., Hamedi, M. M., and Wågberg, L. (2017). "Understanding the dispersive action of nanocellulose for carbon nanomaterials," *Nano Letters* 17(3), 1439-1447. DOI: 10.1021/acs.nanolett.6b04405

Halperin, W. P. (1986). "Quantum size effects in metal particles," *Reviews of Modern Physics* 58(3), 533-606. DOI: 10.1103/RevModPhys.58.533

Hu, Z., Fu, S., and Tang, A. (2017a). "Fabrication of light-triggered AuNP/CNC/SMP nano-composites," *BioResources* 12(1), 1982-1990. DOI: 10.15376/biores.12.1.1982-1990

*bioresources*.com

Hu, Z., Meng, Q., Liu, R., Fu, S., and Lucia, L. A. (2017b). "Physical study of the primary and secondary photothermal events in gold/cellulose nanocrystals (AuNP/CNC) nanocomposites embedded in PVA matrices," *ACS Sustainable Chemistry & Engineering* 5(2), 1601-1609. DOI: 10.1021/acssuschemeng.6b02380

Koga, H., Tokunaga, E., Hidaka, M., Umemura, Y., Saito, T., Isogai, A., and Kitaoka, T. (2010). "Topochemical synthesis and catalysis of metal nanoparticles exposed on crystalline cellulose nanofibers," *Chemical Communications* 46(45), 8567-8569. DOI: 10.1039/C0CC02754E

Leng, W., Pati, P., and J. Vikesland, P. J., (2015). "Room temperature seed mediated growth of gold nanoparticles: Mechanistic investigations and life cycle assesment," *Environmental Science: Nano* 2(5), 440-453. DOI: 10.1039/C5EN00026B

Lopez, N., Janssens, T. V. W., Clausen, B. S., Xu, Y., Mavrikakis, M., Bligaard, T., and Nørskov, J. K. (2004). "On the origin of the catalytic activity of gold nanoparticles for low-temperature CO oxidation," *Journal of Catalysis* 223(1), 232-235. DOI: 10.1016/j.jcat.2004.01.001

Marques, L., Hernandez, F. U., James, S. W., Morgan, S. P., Clark, M., Tatam, R. P., and Korposh, S. (2016). "Highly sensitive optical fibre long period grating biosensor anchored with silica core gold shell nanoparticles," *Biosensors and Bioelectronics* 75, 222-231. DOI: 10.1016/j.bios.2015.08.046

Milone, C., Ingoglia, R., Neri, G., Pistone, A., and Galvagno, S. (2001). "Gold catalysts for the liquid phase oxidation of o-hydroxybenzyl alcohol," *Applied Catalysis A: General* 211(2), 251-257. DOI: 10.1016/S0926-860X(00)00875-9

Mittal, N., Jansson, R., Widhe, M., Benselfelt, T., Håkansson, K. M. O., Lundell, F., Hedhammar, M., and Söderberg, L. D. (2017). "Ultrastrong and bioactive nanostructured bio-based composites," *ACS Nano* 11(5), 5148-5159. DOI: 10.1021/acsnano.7b02305

Panigrahi, S., Basu, S., Praharaj, S., Pande, S., Jana, S., Pal, A., Ghosh, S. K., and Pal, T. (2007). "Synthesis and size-selective catalysis by supported gold nanoparticles: Study on heterogeneous and homogeneous catalytic process," *The Journal of Physical Chemistry C* 111(12), 4596-4605. DOI: 10.1021/jp067554u

Paukkonen, H., Kunnari, M., Laurén, P., Hakkarainen, T., Auvinen, V. V., Oksanen, T., Koivuniemi, R., Yliperttula, M., and Laaksonen, T. (2017). "Nanofibrillar cellulose hydrogels and reconstructed hydrogels as matrices for controlled drug release," *International Journal of Pharmaceutics* 532(1), 269-280. DOI: 10.1016/j.ijpharm.2017.09.002

Shi, C., Zhu, N., Cao, Y., and Wu, P. (2015). "Biosynthesis of gold nanoparticles assisted by the intracellular protein extract of *Pycnoporus sanguineus* and its catalysis in degradation of 4-nitroaniline," *Nanoscale Research Letters* 10(1), 147. DOI: 10.1186/s11671-015-0856-9

Siddiqi, K. S., and Husen, A. (2017). "Recent advances in plant-mediated engineered gold nanoparticles and their application in biological system," *Journal of Trace Elements in Medicine and Biology* 40, 10-23. DOI: 10.1016/j.jtemb.2016.11.012

Tian, C., Fu, S., Chen, J., Meng, Q., and Lucia, L. A. (2014). "Graft polymerization of ε-caprolactone to cellulose nanocrystals and optimization of grafting conditions utilizing a response surface methodology," *Nordic Pulp & Paper Research Journal* 29(1), 58-68. DOI: 10.3183/npprj-2014-29-01-p058-068

Turkevich, J., Stevenson, P. C., and Hillier, J. (1951). "A study of the nucleation and growth processes in the synthesis of colloidal gold," *Discussions of the Faraday Society* 11, 55-75. DOI: 10.1039/DF9511100055

Veith, G. M., Lupini, A. R., Pennycook, S. J., Ownby, G. W., and Dudney, N. J. (2005). "Nanoparticles of gold on γ-Al$_2$O$_3$ produced by dc magnetron sputtering," *Journal of Catalysis* 231, 151-158. DOI: 10.1016/j.jcat.2004.12.008

Xiong, R., Kim, H. S., Zhang, L., Korolovych, V. F., Zhang, S., Yingling, Y. G., and Tsukruk, V. V. (2018). "Wrapping nanocellulose nets around graphene oxide sheets," *Angewandte Chemie International Edition* 57(28), 8508-8513. DOI: 10.1002/anie.201803076

Xu, Y., Li, S., Yue, X., and Lu, W. (2017). "Review of silver nanoparticles (AgNPs)-cellulose antibacterial composites," *BioResources* 13(1), 2150-2170. DOI: 10.15376/biores.13.1.Xu

Yan, W., Chen, C., Wang, L., Zhang, D., Li, A. J., Yao, Z., and Shi, L. Y. (2016). "Facile and green synthesis of cellulose nanocrystal-supported gold nanoparticles with superior catalytic activity," *Carbohydrate Polymers* 140, 66-73. DOI: 10.1016/j.carbpol.2015.12.049

Zhang, H., Yang, H., Chen, H. J., Du, X., Wen, D., and Wu, H. (2017). "Photothermal conversion characteristics of gold nanoparticles under different filter conditions," *Energy* 141, 32-39. DOI: 10.1016/j.energy.2017.09.059

Zhang, H., and Zhao, Y. (2013). "Polymers with dual light-triggered functions of shape memory and healing using gold nanoparticles," *ACS Applied Materials & Interfaces* 5(24), 13069-13075. DOI: 10.1021/am404087q

Zhang, K., Shen, M., Liu, H., Shang, S., Wang, D., and Liimatainen, H. (2018). "Facile synthesis of palladium and gold nanoparticles by using dialdehyde nanocellulose as template and reducing agent," *Carbohydrate Polymers* 186, 132-139. DOI: 10.1016/j.carbpol.2018.01.048